Modelling growth of northern krill (*Meganyctiphanes norvegica*) using an energy-budget approach*

Tjalling Jager[a], Elisa Ravagnan[b]

[a] *DEBtox Research, De Bilt, the Netherlands*
[b] *IRIS Environment, International Research Institute of Stavanger, Postboks 8046, N-4068 Stavanger, Norway*

Abstract

Northern krill (*Meganyctiphanes norvegica*) is an important species in the North Atlantic and the Mediterranean Sea, but very little life-history information is available under controlled (laboratory) conditions. Here, we use the DEBkiss model to piece together the available data into a quantitative energy budget. We use this model to analyse larval growth curves, and to reconstruct the feeding history for field populations from their (reconstructed) multi-year growth patterns. The resulting model parameters are also used to provide estimates for respiration, feeding and reproduction rates that are consistent with measured values. Many uncertainties remain, but this analysis demonstrates how simple and generic energy-budget models have the potential to integrate observations on different traits, to interpret growth as a function of food and temperature, and to compare different species in a meaningful manner.

Keywords: Dynamic Energy Budget, DEBkiss, *Meganyctiphanes norvegica*, life-history traits, growth modeling, krill

Email address: tjalling@debtox.nl (Tjalling Jager)
URL: http://www.debtox.nl/ (Tjalling Jager)

1. Introduction

Krill forms a large part of the marine zooplankton, and a quantitative understanding of their life histories is important to predict their responses to a changing environment, and to protect populations from anthropogenic impacts. Dynamic Energy Budget (DEB) theory (Nisbet et al., 2000) is a valuable framework in this respect, as it links the acquisition of energy from the environment (feeding) to energy-requiring processes (growth, reproduction, etc.) over the entire life cycle. A simplified model from this framework, DEBkiss (Jager et al., 2013), has been quite succesful to interpret and to predict life-history traits of invertebrate animals as a function of environmental conditions and exposure to stressors (e.g., Jager and Ravagnan, 2015; Barsi et al., 2014; Jager et al., 2015). The complete calibration of DEBkiss, however, still requires a substantial input of life-history data (especially observations on growth and reproduction) over a substantial part of the life cycle, under controlled (or at least well known) conditions. For krill, laboratory data on growth and reproduction are scarce, as the species are long lived and most of them do not cope well with laboratory conditions (Nicol, 2000). Earlier, we pieced together the available data for the Antarctic krill (*Euphausia superba*) for a parameterisation of DEBkiss (Jager and Ravagnan, 2015). However, due to the lack of data on lipid storage and reproduction under controlled conditions, even for this species, the analysis had to be considered a provisional one.

For the northern krill (*Meganyctiphanes norvegica*), even less data is available; for example, we have not been able to locate a growth curve for post-larval stages under laboratory conditions. What is available, however, is laboratory growth data on larvae over the calyptopis and furcilia stages (Le Roux, 1974), and several reconstructed growth curves based on size measurements of field-collected specimens (Cuzin-Roudy et al., 2004; Boysen and Buchholz, 1984; Labat and Cuzin-Roudy, 1996). The question we address in this study is whether this scattered data can be used to parameterise DEBkiss, and what we can learn from this model about growth in the field under time-varying temperature and food availability. More specifically, we will parameterise the model using key elements from the reconstructed growth curves and the larval growth data under laboratory conditions. Next, we provide a reality check by comparing model predictions to measured data for other traits (feeding, respiration and reproduction), and use growth curves from field populations to reconstruct their feeding history. In earlier work,

DEB models proved to be powerful tools for such reconstructions (see e.g., Freitas et al., 2009; Pecquerie et al., 2012).

The use of a generic energy-budget model implies that many 'details' on the life history will inevitably be lost. What we gain, however, is generality. For example, we do not need to start from scratch when moving from one species to another, making DEB-based models an efficient building block for individual-based population models (Martin et al., 2012). More recently, elements from DEBkiss were used in an individual-based model for Antarctic krill (Groeneveld et al., 2015). Furthermore, the generality of the DEBkiss framework allows us to make meaningful comparisons between northern krill and other krill species such as Antarctic krill (Jager and Ravagnan, 2015), but also other crustaceans such as copepods (Jager et al., 2015), or even quite unrelated species such as freshwater snails (Barsi et al., 2014). Apart from the relevance for northern krill ecology, this study is therefore also a demonstration how simple, generic, models for the energy budget can aid the interpretation of life-history data.

2. Methods

2.1. Basic model equations

The DEBkiss model is schematically shown in Fig. 1, and has been described in detail elsewhere (Jager et al., 2013; Jager, 2015). The model equations for growth can be rewritten to the von Bertalanffy growth curve; as a differential equation for the physical length (L_w) of the organism as function of the food level (f):

$$\frac{d}{dt}L_w = r_B(fL_{wm} - L_w) \quad \text{with } L_w(0) = L_{w0} \tag{1}$$

Where f is the scaled functional response ($f = 1$ marks *ad libitum* feeding and $f = 0$ is complete starvation). The two remaining parameters are L_{wm}, the maximum physical length at abundant food, and r_B the von Bertalanffy growth rate constant. This differential equation can be solved analytically when all parameters are constant. However, as we want to apply the model to time-varying food and temperature situations, we stick to the differential equation here.

Temperature (T) is assumed to affect all physiological rate constant by the same factor F_T, following from the Arrhenius relationship:

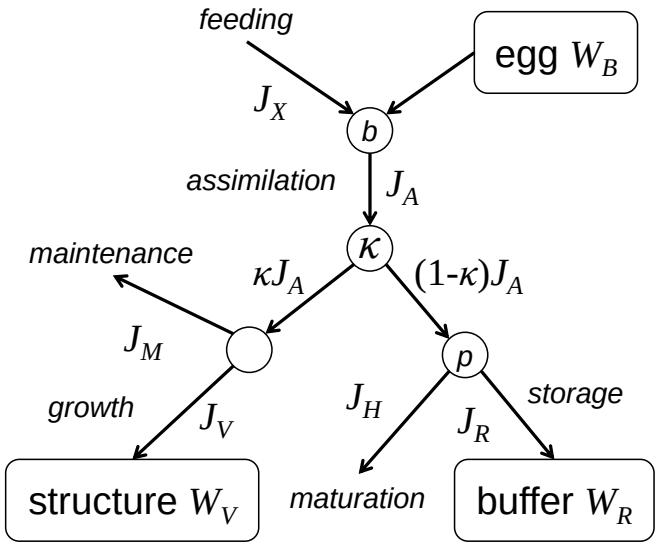

Figure 1: Diagram of the DEBkiss model with all state variables (the masses W_i) and mass fluxes (J_i). The κ node represents the allocation of the assimilation flux to the soma (structural tissues and its maintenance needs) with a fixed fraction κ. The remaining fraction $(1-\kappa)$ is allocated to maturation or the reproduction buffer. The buffer is used to pay maintenance costs under starvation, and to fuel gonad maturation and reproduction. The node b represents the switching on of feeding at 'birth', and the node p represents a switch from maturation to reproduction buffer at 'puberty'.

$$F_T = \exp\left(\frac{T_A}{T_{ref}} - \frac{T_A}{T}\right) \tag{2}$$

Where T_A is known as the Arrhenius temperature, and T_{ref} is a reference temperature (all in Kelvin).

The model parameters r_B and L_{wm} from Eq. 1 are compound parameters that are determined by more basic parameters of the energy budget (the primary parameters). The von Bertalanffy rate constant r_B relates to the volume-specific maintenance costs (J_M^v) of the organism (Jager et al., 2013):

$$r_B = \frac{y_{VA}}{3d_V} J_M^v \tag{3}$$

Where y_{VA} is the yield of body structure on assimilates, and d_V the dry weight of structure per unit of structural volume (numerically equivalent to the dry/wet weight ratio). The maximum length follows from the primary parameters as follows:

$$L_{wm} = \frac{\kappa J_{Am}^a}{\delta_M J_M^v} \tag{4}$$

Where κ is the fraction of the assimilation flux allocated to the soma (structural growth and maintenance, see Fig. 1), J_{Am}^a is the maximum area-specific assimilation rate, and δ_M is the shape correction coefficient to translate actual body length to volumetric body length (the cubic root of volume).

2.2. Model predictions

If we set reasonable default values for the additional model parameters and conversion factors, we can use the estimates for L_{wm} and r_B to calculate primary parameters of the energy budget, and use those to predict other physiological traits of the species, such as respiration, feeding rates, and reproductive output (see Jager and Ravagnan, 2015).

Oxygen use is related to the sum of a number of dissipating mass fluxes, mainly maintenance (J_M), maturation (J_H), and the overhead costs for growth (J_{Vo}) and reproduction (J_{Ro}). Ignoring the contribution of the latter process (which is rather small, and only relevant in females when eggs are being prepared), these fluxes (in mg/d) are specified as functions of the volumetric body length ($L = \delta_M L_w$) as follows (Jager et al., 2013; Jager, 2015):

$$J_M = J_M^v L^3 \quad (5)$$
$$J_H = (1-\kappa) f J_{Am}^a L^2 \quad (6)$$
$$J_{Vo} = (1-y_{VA}) \left(\kappa f J_{Am}^a L^2 - J_M^v L^3\right) \quad (7)$$

Maturation is the process by which assimilates are burnt to increase the complexity of the organism, and which thus contributes to the respiration flux. At 'puberty', this flux is assumed to switch to the reproduction buffer (see Fig. 1).

The dissipation fluxes are in mg dry weight of assimilates or body weight per day (in DEBkiss, assimilates and structure are assumed to have a similar composition, so for the respiration predictions, the difference can be ignored). This can be converted into carbon fluxes by multiplying with the weight of carbon per unit of dry body weight (d_C), to moles using the molar weight of carbon, and subsequently to moles of O_2 assuming a respiration quotient of 0.9 (as was used in Jager and Ravagnan, 2015). The fluxes will be expressed per dry weight of animal by dividing by the dry body weight:

$$W_V = d_V L^3 \quad (8)$$

It should be noted that W_V is the structural body weight. Krill will build up a seasonal lipid storage (see e.g., Båmstedt, 1976), and since such a storage is not expected to require maintenance, this process may bias the comparison between observed respiration rates and model prediction to some extent (see Jager and Ravagnan, 2015).

The maximum specific assimilation rate can be used to estimate the feeding rate in mg dry weight of food per day (see Jager and Ravagnan, 2015):

$$J_X = \frac{f J_{Am}^a L^2}{y_{AX}} \quad (9)$$

Where y_{AX} is the assimilation efficiency from food. Similar to the respiration rates, the feeding rate will also be expressed per unit of body weight (again, with a potential bias if the body mass of the experimental animals included a considerable lipid storage).

For krill, we propose to view the seasonal lipid storage as (part of) the reproduction buffer (see Fig. 1). At 'puberty', the $1-\kappa$ flux of assimilates is shifted from maturation to storage, which can be used both for surviving

seasonal episodes of poor food availability and for fuelling egg production. At this moment, it is not clear at which life stage this switch occurs, and whether it is complete and definitive (Jager and Ravagnan, 2015). Furthermore, the rules for handling this reproduction buffer cannot yet be established, i.e., deciding when to spawn, how much of the buffer to convert into eggs, and when to stop spawning to build up sufficient storage for the next unfavourable season. In the complete absence of data on storage and reproduction under controlled conditions, it is difficult to make realistic predictions for this aspect of krill life history (some energetic constraints are presented in the supporting information). What we can do, however, is to check whether reported estimates for the size of an egg batch and the spawning interval are energetically feasible with our parameterisation. For adults, the flux of resources into the reproduction buffer (J_R), can be translated into a continuous egg production rate (R, in eggs/day):

$$J_R = (1-\kappa) f J_{Am}^a L^2 \tag{10}$$

$$R = J_R \frac{y_{BA}}{W_{B0}} \tag{11}$$

This calculation rests on the assumption that the entire $1-\kappa$ flux is converted into eggs. Krill, however, do not reproduce continuously, but rather spawn large batches of eggs during the reproductive season. An estimate for the number of eggs in a single batch can be obtained by multiplying R with the number of days over which the batch is built up.

2.3. Reconstructing feeding history

Several growth curves under field conditions have been pieced together from field-collected animals in three locations: the Kattegat (Boysen and Buchholz, 1984), Clyde Sea (Cuzin-Roudy et al., 2004), and the Ligurian Sea (Labat and Cuzin-Roudy, 1996). However, only the Kattegat analysis is discussed in the main text; the other two sets are presented in the supporting information.

We can use these growth curves to reconstruct the scaled functional response (f, see Eq. 1) that the animals must have experienced in the field over the year. To do this, we need to know the relevant temperature profile over the year. The water temperature, however, not only varies over time but also with depth (especially during summer). Krill reside in deep water during the day, but come up to the surface layers at night, although their abundance in

the uppermost layer is generally low (Tarling et al., 1999). Saborowski et al. (2000) assumed that krill are subjected to surface temperatures for 6 hours per day, and to deep water temperatures for the remaining 18 hours. We can use the temperature profiles of Saborowski et al. (2002) to construct a representative exposure temperature range. As a pragmatic choice, we calculated a weighted average between the temperature at 25 m depth (weight 1) and 100 m (weight 3) for summer and winter. Assuming that the minimum temperature occurs at 1 February, and the maximum at 1 August, we used a sine function to represent daily temperature.

To present the model animal with a scaled functional response f as a continuous function of time, we used a cubic spline specified by nodes at regular intervals (every 100 days). All nodes are simultaneously fit to the body size data, given the representative temperature profile over the year. This analysis is based on the assumption that growth strictly follows the von Bertalanffy model (Eq. 1), with the same parameter values in each population, and that the only differences in growth are caused by temperature (Eq. 2) and feeding situation (Eq. 1).

2.4. Data treatment, modelling and statistics

Data were extracted from the graphs in the original publications using the freeware PlotReader (`http://jornbr.home.xs4all.nl/plotreader`). The respiration data compiled by Tremblay et al. (2014) were obtained from the supplement to the original publication. The model was implemented in Matlab using the BYOM platform (`http://www.debtox.info/byom.html`). For fitting, a likelihood function was optimised, assuming independent and normally-distributed errors. Confidence intervals on parameter estimates were generated by profiling the likelihood function. For the credible intervals on model outputs, we took a Bayesian perspective, sampling from the posterior distribution (2000 samples, using uniform priors).

3. Results and discussion

3.1. Parameterising the model

In the absence of growth curves for northern krill under controlled conditions, the three parameters of the von Bertalanffy model (Eq. 1) need to be established in a cruder way. We can fix $L_{wm} = 45$ mm, which is a reasonable maximum size for the species (see Tarling, 2010). The r_B can now be established from the growth rate (see Eq. 3), as long as f is known. This is

a problem here as the growth curves that we have are from the field, where food level is unknown, and not necessarily *ad libitum*. The larval growth data of Le Roux (1974) are from the laboratory, but the larvae may grow slower than predicted from the curves for the juveniles/adults (as was the case for Antarctic krill, Jager and Ravagnan, 2015).

As a practical solution, we looked at the steepest growth curve as reconstructed from field-collected animals, which is the one in Clyde Sea, as reported by Cuzin-Roudy et al. (2004). Steepest growth is around the first two summer data points. If we can assume *ad libitum* food ($f = 1$) here, the absolute growth rate (dL_w/dt in mm/d) can be translated into $r_B = 0.0062$ 1/d using Eq. 1. We assume a temperature of 9°C for this growth rate (the representative summer temperature in the Clyde Sea, see methods section).

We need additional model parameters and conversion factors to translate the von Bertalanffy parameters to the underlying energy-budget parameters, and to predict respiration and feeding rates. The dry weight density (d_V) and carbon content (d_C) were taken from the data collection of Brey et al. (2010, conversions databank version 4 of 2012). The shape correction (δ_M) could be derived from the regression between dry weight and total body length in Lindley et al. (1999), using Eq. 8 to convert dry weights to volumetric length. The assimilation efficiency was taken from Fowler and co-workers, as cited by Heyraud (1979). For y_{BA}, y_{VA} and κ, defaults are used (Jager et al., 2013). Egg dry weight (W_{B0}) was calculated from the fresh weight reported by Cuzin-Roudy (2010) and the established value for d_V. All fixed parameters and conversion factors are summarised in Table 1.

Using a fixed value for κ does not influence the goodness-of-fit of the model on growth data (as κ is not part of Eq. 1). However, the values for the underlying energy-budget parameters (particularly J^a_{Am}) will depend on the choice of κ (see Eq. 4), and hence, the absolute parameter values need to be treated with care. Precise estimation of κ requires information on the investment into the $1 - \kappa$ branch, i.e., on the build up of the reproduction buffer under well-known conditions (specifically, food and temperature). Such information is lacking for northern krill, but the model predictions for feeding rate and size of egg batches (see Section 3.3) can shed some light on the suitability of the default used.

Using a fixed value for the shape parameter (δ_M) implies that we assume isomorphic growth, i.e., that structural body weight is proportional to physical length cubed. For Antarctic krill, this was found to be a good approximation, at least for the feeding stages (Jager and Ravagnan, 2015).

Table 1: Fixed parameters and conversion factors in this study.

Symbol	Explanation	Value	unit
d_C	fraction carbon in dry weight	0.42	mg mg^{-1} (dwt.)
d_V	dry weight density of structure	0.21	mg mm^{-3}
L_{wm}	maximum length	45	mm
r_B	von Bertalanffy rate constant	0.0062	d^{-1}
T_{ref}	reference temperature (9°C)	282	K
W_{B0}	dry weight of a single egg	0.0076	mg (dwt.)
y_{AX}	yield of assimilates on food	0.76	mg mg^{-1} (C)
y_{BA}	yield of egg buffer on assimilates	0.95	mg mg^{-1} (dwt.)
y_{VA}	yield of structure on assimilates	0.8	mg mg^{-1} (dwt.)
δ_M	shape correction coefficient	0.21	(-)
κ	allocation fraction to the soma	0.8	(-)

In practice, weight-length relationships may deviate from isomorphism when animals with a considerable storage are included (storage is not part of structure in the model).

3.2. Fitting larval growth data

Data were extracted from Le Roux (1974), who studied larval growth (calyptopis and furcilia stages) in four different food treatments and at two temperatures (Fig. 2). These data were fitted with the von Bertalanffy model of Eq. 1, with parameters r_B and L_m fixed as in Table 1, and the temperature effect of Eq. 2. This provides estimates for the scaled functional response f in each food treatment, and the Arrhenius temperature T_A (Table 2).

The estimates for the scaled functional response f are considerably lower than 1, even for the best food treatment in this experiment (Table 2). This could point at experimental problems, such as a sub-optimal food source for these stages (see Zimmer et al., 2012). However, initial slow growth is observed in a range of species, and may indicate a form of metabolic acceleration over the life cycle (Kooijman, 2014). For example, a step-up of assimilation at the start of the juvenile stage (type A acceleration) may explain the observed discrepancy. In Antarctic krill, the larval period was also longer than predicted from the growth rate of the juveniles/adults (Jager and Ravagnan, 2015). In that case, however, this appeared to be specifically due to a slow growth rate in the furcilia stages (and not for the calyptopis

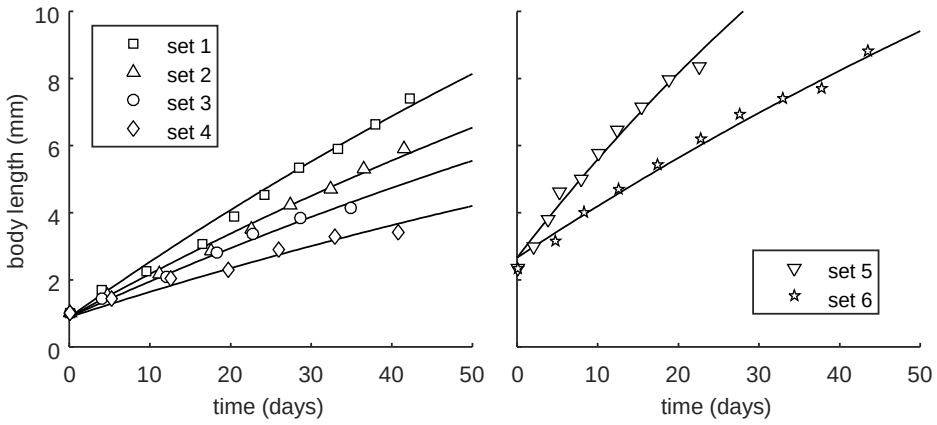

Figure 2: Fitting larval growth data for four different feeding regimes (left panel, 10°C, food regimes specified in Table 2) and two temperatures (right panel, set 5 at 20°C and set 6 at 10°C).

larvae). Such a difference between these two larval types was not apparent for northern krill in the study of Le Roux (1974) (Fig. 2).

3.3. Predicting respiration, feeding and reproduction

Using the model parameters from Tables 1 and 2, we can predict respiration, feeding and reproduction rates as a function of body size and temperature. Respiration has contributions from various processes, notably maintenance (Eq. 5), maturation (Eq. 6) and growth overheads (Eq. 7). What we measure as respiration depends on the life stage and the experimental design. For adults, maturation ceases and the allocated energy is not dissipated anymore but stored in the reproduction buffer. During respiration measurements, animals are generally not fed, and at some point, growth will stop (and therefore also the dissipated overheads of growth). The minimum respiration rate is represented by the maintenance costs only, although maintenance needs may be reduced on prolonged starvation (Ikeda and Dixon, 1982) or in response to light regime (Teschke et al., 2007). In Fig. 3, we plot three predictions to indicate the range of respiration rates that can be expected from the model parameterisation (the maximum rate is based on the sum of the three above-mentioned dissipation fluxes).

For respiration, we used the data from Saborowski et al. (2002) for males from three locations, incubated at different temperatures. The reported respiration rates had been scaled allometrically to a standard body length of 30

Table 2: Model parameters estimated from the von Bertalanffy parameters and the larval growth data. For the latter fit (see Fig. 2), parameters are shown with 95% confidence intervals.

Symbol	Explanation	Value	unit
J^a_{Am}	specific max. assimilation rate	0.058	mg mm^{-2} d^{-1}
J^v_M	specific maintenance rate	0.0049	mg mm^{-3} d^{-1}
f	scaled functional response		
	Artemia and algae (set 1, 5, 6)	0.59 (0.57-0.61)	(-)
	Artemia only (set 2)	0.46 (0.44-0.48)	(-)
	algae only, every day (set 3)	0.39 (0.36-0.41)	(-)
	algae every other day (set 4)	0.28 (0.26-0.30)	(-)
L_{w0}	initial body length, set 1-4	0.88 (0.78-0.98)	mg (dwt.)
	initial body length, set 5-6	2.7 (2.5-2.8)	mg (dwt.)
T_A	Arrhenius temperature	5630 (5110-6140)	K

mm, and are plotted in the left panel of Fig. 3. The differences between the data sets are not so easy to interpret (a larger plot with legend is provided in the supporting information), but the purpose here is to demonstrate that the model parameters provide estimates that are in the right range, and that the temperature dependence is captured well. The right plot of Fig. 3 shows respiration data compiled by Tremblay et al. (2014) for *M. norvegica*. We converted all data to a reference temperature of 9°C using the Arrhenius temperature of Table 2. The spread in the data is considerable, but the model predictions are within the range of the measured data, providing support for the model parameterisation.

In Fig. 4, the feeding rate measurements from Heyraud (1979) and Båmstedt and Karlson (1998) are combined. These data were derived at 13 and 10-12°C), respectively, so we took 12°C for the temperature conversion. It should be stressed that the prediction for the feeding rate is quite sensitive to values of κ and y_{AX}. For κ, a general default was used (Jager et al., 2013), but this value may vary considerably between species (see Kooijman, 2013). The spread in the data is very large, likely reflecting the experimental difficulties of measuring feeding rates. However, the prediction is in the correct range, albeit at the lower end of that range. Some of the higher measured values may have resulted from a bias if prey is only partially eaten (Båmstedt and Karlson, 1998).

The predicted reproduction rate (Eq. 11) cannot be directly compared

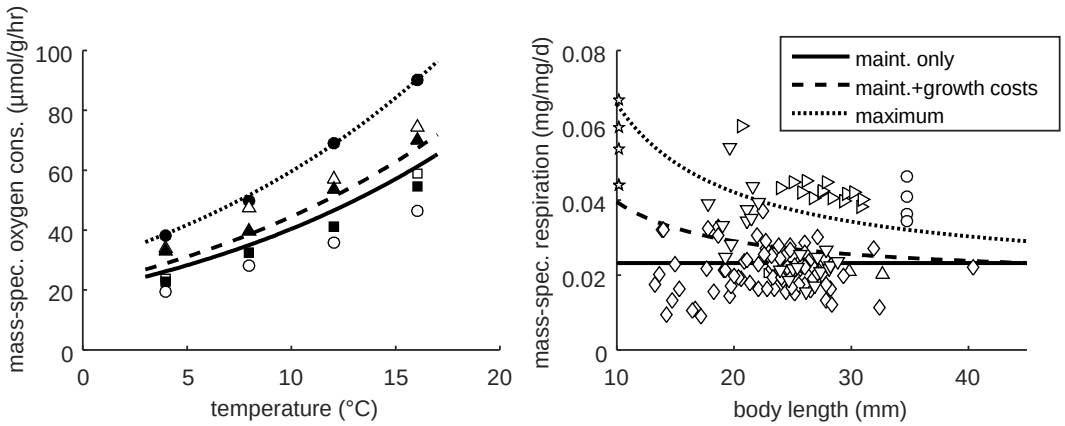

Figure 3: Predicted (Eq. 5-7) and measured respiration rates for krill. Left panel, data from Saborowski et al. (2002), who corrected values to a body size of 30 mm. Right panel, data from Tremblay et al. (2014) that we corrected to a temperature of 9°C. Different symbols represent different data sets (see supp. info. for details).

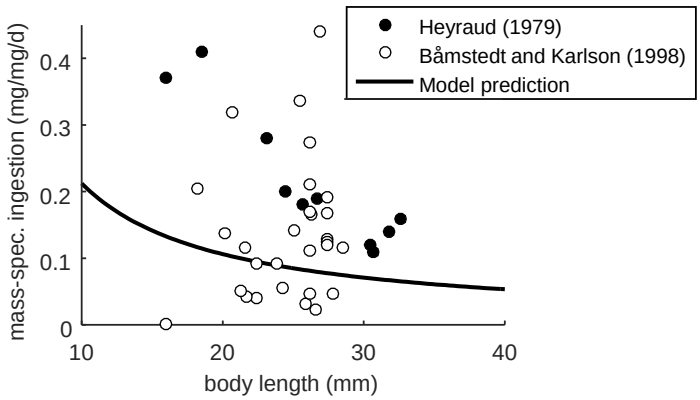

Figure 4: Predicted (Eq. 9) and measured ingestion rates for krill. Model prediction is for *ad libitum* feeding and 12°C, which is close to the temperature used in both experimental studies.

to measured data; in the laboratory, krill do not go through multiple spawning cycles. A more indirect comparison is, however, feasible. Cuzin-Roudy (2000) determined the number of mature oocytes in individuals sampled from the field (same locations as those used for the reconstructions of the feeding history). These oocyte counts likely reflect the size of an egg batch at a spawning event, and are plotted versus body length in Fig. 5. To compare these batch sizes to the model estimates for the reproduction rate, we need the time between subsequent spawning events. Based on the estimates of Cuzin-Roudy (2000), we use two scenarios for our predicted batch size: a scenario representative for the Ligurian Sea (13°C, and 15 days between spawning events) and one for the Kattegat (8°C, and 30 days between spawning events). For the feeding conditions, we assume *ad libitum* food availability ($f = 1$); the estimated batch size is thus the maximum possible for the defined temperature and spawning interval.

The results in Fig. 5 show that the majority of the observed numbers of mature oocytes, in conjunction with the estimated spawning intervals, are consistent with the model predictions. Lower-than-expected oocyte counts can easily be explained by sub-optimal feeding conditions. Individuals with higher oocyte counts may have had a longer spawning interval. However, we should also consider that part of the energy for building the first batch(es) of eggs of the reproductive season may have resulted from the storage remaining after the non-reproductive period. The general correspondence between model predictions and data supports a value for κ close to the default of 0.8.

3.4. Reconstructing feeding history

We can now use the von Bertalanffy model of Eq. 1 and 2, with the parameters in Table 2, to analyse the growth patterns derived for field populations over multiple years. If we apply a reasonable temperature profile for each field site, we can reconstruct the feeding history from data on body length versus age (see methods section). Only the reconstruction for the Kattegat (data from Boysen and Buchholz, 1984) is shown here in Fig. 6; the other two reconstructions can be found in the supporting information. The reconstructed scaled functional response (f) in the Kattegat varies seasonally, although within a rather narrow range. Also shown in Fig. 6 is the predicted growth curve for continuous *ad libitum* conditions ($f = 1$). This shows that the influence of the fluctuating temperature over the year is small, and that the growth curve is mainly influenced by the feeding situation.

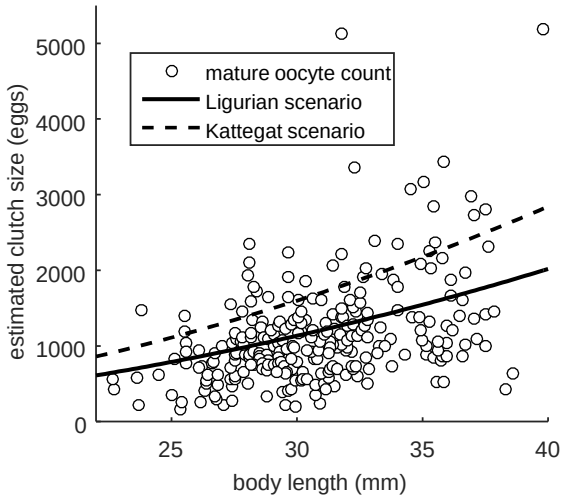

Figure 5: Number of mature oocytes (as proxy for the size of an egg batch) versus body length; data from Cuzin-Roudy (2000). Model predictions from Eq. 11 assuming *ad libitum* feeding; temperature and spawning interval according to two scenarios (see text).

In winter, a considerable amount of feeding apparently still occurs, as the predicted f does not fall below 0.5. This is a consequence of using the growth model of Eq. 1: lower values of f would lead to shrinking ($dL_w/dt < 0$), which was not observed in the data set. However, this equation does not consider the possibility that the lipid storage may prevent shrinking during winter. Therefore, we performed another reconstruction in which shrinking was avoided by forcing $dL_w/dt >= 0$ in Eq. 1 (Fig. 7). This analysis represents the situation where the storage is always sufficient to cover the maintenance needs, and thus prevents shrinking. With this additional assumption, the uncertainty surrounding the food situation in winter becomes much larger. The uncertainty also increases dramatically at the end of the data set; as the animals are approaching their asymptotic size, the growth rate becomes less sensitive to the food level (as long as we don't allow shrinking). Without observations on body weight and composition (to differentiate between structure and storage), we have little possibility to decrease the confidence intervals on the reconstructed feeding history.

Boysen and Buchholz (1984) also report chlorophyll *a* content at 10-meter depth over the year, as a measure of phytoplankton concentration. This parameter shows clear peaks in spring and autumn, which are not prevalent in the reconstructions for the feeding history. It should be stressed that our

reconstruction reflects what is eaten (or more accurately, assimilated) rather than what is available as phytoplankton. Feeding rates may already have saturated at relatively low food concentrations, krill (particularly the larger individuals) also feed on non-phytoplankton items, and during winter, feeding rates may well be low even when sufficient food is present (see Teschke et al., 2007, for Antarctic krill).

The estimated f over the first 50 days is quite low (0.4-0.6), compared to the estimates for the 1- and 2-year older individuals in the same time of year (summer). These are small individuals (4-8 mm), and therefore likely to be furcilia larvae. Interestingly, this is consistent with the low estimated f for the larvae under laboratory conditions (Fig. 2, Table 2). This observation thus strengthens the hypothesis that the slow initial growth is a physiological property of the species, and not an experimental artefact.

We assume that growth is only influenced by food and temperature, but that the energy-budget parameters are the same for each population. This assumption is debatable, especially considering the work of Saborowski et al. (2002), who provides a clear indication that populations can, over the long term, adapt their physiology to local conditions. It would thus be very interesting to study animals from different populations under controlled conditions, to see if and how their energy-budget parameters differ.

3.5. Comparison to other species

We can now compare the parameters established for *M. norvegica* to other species that have been analysed with DEBkiss (Table 3), as the parameters have exactly the same interpretation. To facilitate the comparison, we also recalculated the rate parameters to a common temperature. However, these results need to be interpreted with care, as species may have adapted to the environmental temperatures in their natural habitat (see Saborowski et al., 2002).

The specific maintenance (J_M^v) and assimilation (J_{Am}^a) rates are larger for *M. norvegica*, than for *E. superba*. However, after accounting for the difference in reference temperature, the rates are quite similar. The larger body size of *E. superba* is mainly explained from a higher assimilation rate, rather than a reduced maintenance. The rate parameters for both krill species are strikingly similar to the values for the pond snail *Lymnaea stagnalis* (after temperature correction). These species have a rather similar size (in terms of structural body volume), but are only very distantly related. Comparing the krill species to the copepod *Calanus sinicus*, it is striking that the specific

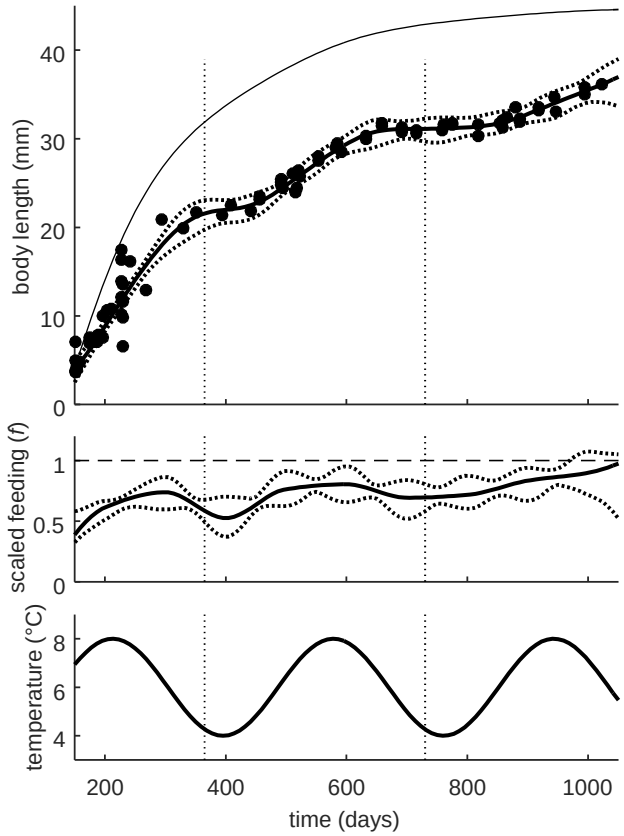

Figure 6: Reconstruction of the feeding history (i.e., scaled functional response f, middle plot) for krill in the Kattegat, based on observed size at age (top plot). Thin line shows the predicted growth curve for constant *ad libitum* food availability. Bottom plot shows the assumed temperature profile. Apart from f, the only parameter estimated is the initial length ($L_{w0} = 4.1$ mm).

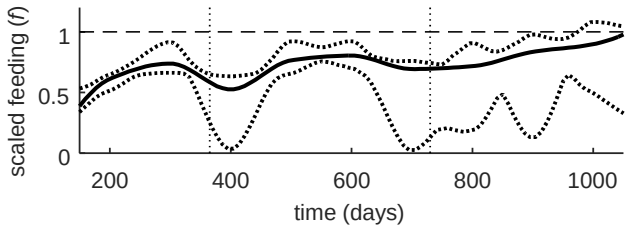

Figure 7: Alternative reconstruction of the feeding history (i.e., scaled functional response f) for krill in the Kattegat, based on the assumption that krill do not shrink in winter due to their lipid storage.

Table 3: Comparing the main energy-budget parameters among different species: northern Krill (*M. norvegica*), Antarctic krill (*Euphausia superba*), a copepod (*Calanus sinicus*), a springtail (*Folsomia candida*), and the pond snail (*Lymnaea stagnalis*). Values in parentheses are recalculated to a common temperature of 10°C, using Eq. 2, applying the T_A established for each species (for *E. superba* the same value as for *M. norvegica* was assumed, and for *L. stagnalis* a default of 8000 K was used). An asterisk indicates where κ was fixed to a default value. Units for J^a_{Am} are mg mm^{-2} d^{-1}, and for J^v_M mg mm^{-3} d^{-1}.

Species	J^a_{Am}	J^v_M	κ	T_{ref}	Reference
M. norvegica	0.058 (0.062)	0.0049 (0.0053)	0.8*	9°C	this study
E. superba	0.044 (0.091)	0.0032 (0.0066)	0.8*	0°C	Jager and Ravagnan (2015)
C. sinicus	0.036 (0.036)	0.020 (0.020)	0.8*	10°C	Jager et al. (2015)
F. candida	0.061 (0.027)	0.066 (0.030)	0.78	20°C	Hamda (2014)
L. stagnalis	0.19 (0.066)	0.011 (0.0038)	0.62	21°C	Barsi et al. (2014)

assimilation is not too different, but that the maintenance rate is much higher in the copepod. The copepod is again not very different from the (rather similarly sized) terrestrial springtail *Folsomia candida*, when correcting the rates for the temperature difference.

These comparisons should be treated as preliminary; most data sets are not optimal for calibrating the model, and the values of most conversion factors is not easy to establish. Furthermore, several parameters were fixed in these analyses (including κ in several cases), which also implies a bias in the estimation of the other parameters. However, this table underlines the potential of the energy-budget framework to unify ecological research across taxa. It tentatively indicates that similar-sized species have similar energetics, and that body size (across the range of species in Table 3) is mainly related to differences in specific maintenance needs, although clearly more work is needed to test these trends. Interestingly, Kooijman (2013) found very similar trends in the parameters of the standard DEB model, for a much larger number of animal species, and provides a (speculative but testable) hypothesis to explain it.

4. Conclusions

In this study, we demonstrate how a minimal data set on life history can be used to parameterise the energy budget of northern krill. Large uncertainties remain, especially for the value of κ (the allocation to growth and maintenance, Fig. 1), on the rules for build up and use of lipid storage,

and on the fuelling of the reproductive output. However, the correspondence of the model predictions for feeding, respiration and egg batch size to measured data lends credence to the current parameterisation. The available information was sufficient to allow for a reconstruction of the feeding history (as scaled functional response, f) from growth patterns in the field. Larval stages grow slower than expected from the later stages, which points at some form of metabolic acceleration.

The DEBkiss model provides a simple framework to analyse a diverse range of observations on life-history traits in a consistent and quantitative manner. Furthermore, it provides a solid basis for comparing different species of krill, and even to compare krill to much more distantly related species in a meaningful manner. As such, simple energy-budget models are a useful quantitative tool for ecological research.

5. Acknowledgements

This study was financially supported by the Research Council of Norway through the grant 204023/E40 "Integrated model system: Risk and Ecosystem Based Management of Arctic waters", WP3: "Energetics as a link from sub-individuals to populations."

References

Barsi, A., Jager, T., Collinet, M., Lagadic, L., Ducrot, V., 2014. Considerations for test design to accommodate energy-budget models in ecotoxicology: a case study for acetone in the pond snail *Lymnaea stagnalis*. Environmental Toxicology and Chemistry 33, 1466–1475.

Boysen, E., Buchholz, F., 1984. *Meganyctiphanes norvegica* in the Kattegat. Studies on the annual development of a pelagic population. Marine Biology 79, 195–207.

Båmstedt, U., 1976. Studies on deep-water pelagic community of korsfjorden, western norway. changes in size and biochemical composition of *Meganyctiphanes norvegica* (Euphausiacea) in relation to its life cycle. Sarsia 61, 15–30.

Båmstedt, U., Karlson, K., 1998. Euphausiid predation on copepods in coastal waters of the northeast atlantic. Marine Ecology Progress Series 172, 149–168.

Brey, T., Müller-Wiegmann, C., Zittier, Z.M.C., Hagen, W., 2010. Body composition in aquatic organisms. a global data bank of relationships between mass, elemental composition and energy content. Journal of Sea Research 64, 334–340.

Cuzin-Roudy, J., 2000. Seasonal reproduction, multiple spawning, and fecundity in northern krill, *Meganyctiphanes norvegica*, and Antarctic krill, *Euphausia superba*. Canadian Journal of Fisheries and Aquatic Sciences 57, 6–15.

Cuzin-Roudy, J., 2010. Reproduction in northern krill (*Meganyctiphanes norvegica* Sars). Advances in Marine Biology 57, 199–230.

Cuzin-Roudy, J., Tarling, G.A., Strömberg, J.O., 2004. Life cycle strategies of Northern krill (*Meganyctiphanes norvegica*) for regulating growth, moult, and reproductive activity in various environments: the case of fjordic populations. Ices Journal of Marine Science 61, 721–737.

Freitas, V., Cardoso, J., Santos, S., Campos, J., Drent, J., Saraiva, S., Witte, J.I., Kooijman, S.A.L.M., Van der Veer, H.W., 2009. Reconstruction of food conditions for Northeast Atlantic bivalve species based on Dynamic Energy Budgets. Journal of Sea Research 62, 75–82.

Groeneveld, J., Johst, K., Kawaguchi, S., Meyer, B., Teschke, M., Grimm, V., 2015. How biological clocks and changing environmental conditions determine local population growth and species distribution in antarctic krill (*Euphausia superba*): a conceptual model. Ecological Modelling 303, 78–86.

Hamda, N.T., 2014. Mechanistic models to explore combined effects of toxic chemicals and natural stressing factors: case study on springtails. PhD thesis, Jagiellonian University, Krakow/VU University Amsterdam (http://hdl.handle.net/1871/50121).

Heyraud, M., 1979. Food ingestion and digestive transit time in the euphausiid *Meganyctiphanes norvegica* as a function of animal size. Journal of Plankton Research 1, 301–311.

Ikeda, T., Dixon, P., 1982. Body shrinkage as a possible over-wintering mechanism of the Antarctic krill, *Euphausia superba* Dana. Journal of Experimental Marine Biology and Ecology 62, 143–151.

Jager, T., 2015. DEBkiss. A simple framework for animal energy budgets. Leanpub: https://leanpub.com/debkiss_book, Version 1.4.

Jager, T., Martin, B.T., Zimmer, E.I., 2013. DEBkiss or the quest for the simplest generic model of animal life history. Journal of Theoretical Biology 328, 9–18.

Jager, T., Ravagnan, E., 2015. Parameterising a generic model for the dynamic energy budget of Antarctic krill, *Euphausia superba*. Marine Ecology Progress Series 519, 115–128.

Jager, T., Salaberria, I., Hansen, B.H., 2015. Capturing the life history of the marine copepod *Calanus sinicus* into a generic bioenergetics framework. Ecological Modelling 299, 114–120.

Kooijman, S.A.L.M., 2013. Waste to hurry: dynamic energy budgets explain the need of wasting to fully exploit blooming resources. Oikos 122, 348–357.

Kooijman, S.A.L.M., 2014. Metabolic acceleration in animal ontogeny: an evolutionary perspective. Journal of Sea Research 94, 128–137.

Labat, J.P., Cuzin-Roudy, J., 1996. Population dynamics of the krill *Meganyctiphanes norvegica* (M. Sars, 1857) (Crustacea: Euphausiacea) in the Ligurian Sea (NW Mediterranean sea). Size structure, growth and mortality modelling. Journal of Plankton Research 18, 2295–2312.

Le Roux, A., 1974. Observations sur le développement larvaire de *Meganyctiphanes norvegica* (Crustacea: Euphausiacea) au laboratoire. Marine Biology 26, 45–56.

Lindley, J.A., Robins, D.B., Williams, R., 1999. Dry weight carbon and nitrogen content of some euphausiids from the north Atlantic Ocean and the Celtic Sea. Journal of Plankton Research 21, 2053–2066.

Martin, B.T., Zimmer, E.I., Grimm, V., Jager, T., 2012. Dynamic Energy Budget theory meets individual-based modelling: a generic and accessible implementation. Methods in Ecology and Evolution 3, 445–449.

Nicol, S., 2000. Understanding krill growth and aging: the contribution of experimental studies. Canadian Journal of Fisheries and Aquatic Sciences 57, 168–177.

Nisbet, R.M., Muller, E.B., Lika, K., Kooijman, S.A.L.M., 2000. From molecules to ecosystems through dynamic energy budget models. Journal of Animal Ecology 69, 913–926.

Pecquerie, L., Fablet, R., de Pontual, H., Bonhommeau, S., Alunno-Bruscia, M., Petitgas, P., Kooijman, S.A.L.M., 2012. Reconstructing individual food and growth histories from biogenic carbonates. Marine Ecology Progress Series 447, 151–164.

Saborowski, R., Bröhl, S., Tarling, G.A., Buchholz, F., 2002. Metabolic properties of Northern krill, *Meganyctiphanes norvegica*, from different climatic zones. I. Respiration and excretion. Marine Biology 140, 547–556.

Saborowski, R., Salomon, M., Buchholz, R.F., 2000. The physiological response of Northern krill (*Meganyctiphanes norvegica*) to temperature gradients in the Kattegat. Hydrobiologia 426, 157–160.

Tarling, G.A., 2010. Population dynamics of Northern krill (*Meganyctiphanes norvegica* Sars). Advances in Marine Biology 57, 59–90.

Tarling, G.A., Cuzin-Roudy, J., Buchholz, F., 1999. Vertical migration behaviour in the northern krill *Meganyctiphanes norvegica* is influenced by moult and reproductive processes. Marine Ecology Progress Series 190, 253–262.

Teschke, M., Kawaguchi, S., Meyer, B., 2007. Simulated light regimes affect feeding and metabolism of Antarctic krill, *Euphausia superba*. Limnology and Oceanography 52, 1046–1054.

Tremblay, N., Werner, T., Huenerlage, K., Buchholz, F., Abele, D., Meyer, B., Brey, T., 2014. Euphausiid respiration model revamped: latitudinal and seasonal shaping effects on krill respiration rates. Ecological Modelling 291, 233–241.

Zimmer, E.I., Jager, T., Ducrot, V., Lagadic, L., Kooijman, S.A.L.M., 2012. Juvenile food limitation in standardized tests: a warning to ecotoxicologists. Ecotoxicology 21, 2195–2204.